A Highly Distorted Octahedral d^4 Compound, *cis*-Mo(*t*-BuS)$_2$(*t*-BuNC)$_4$

Masato Kamata,[1a] Ken Hirotsu,[1b] Taiichi Higuchi,[1b] Kazuyuki Tatsumi,[1c] Roald Hoffmann,*[1c] Toshikatsu Yoshida,[1a] and Sei Otsuka*[1a]

Contribution from the Departments of Chemistry, Faculty of Engineering Science, Osaka University, Toyonaka, Osaka 560, Japan, Osaka City University, Sumiyoshiku, Osaka 558, Japan, and Cornell University, Ithaca, New York, 14853. *Received March 16, 1981. Revised Manuscript Received May 18, 1981*

Abstract: The crystal structure of the coordinatively unsaturated d^4 molybdenum complex *cis*-Mo(*t*-BuS)$_2$(*t*-BuNC)$_4$ has been determined by X-ray diffraction. The crystals are monoclinic: a = 18.616 (7) Å, b = 11.823 (2) Å, c = 18.667 (6) Å, β = 116.00 (3)°, space group $P2_1/c$ with four formula weights per unit cell. The structure was refined to R = 0.069 and R_w = 0.086 for 4838 reflections. The six-coordinate molecule is substantially deformed from the ideal octahedral geometry, so that the S–Mo–S and C–Mo–C angles in the equatorial plane are 115.3 (1) and 73.7 (4)°. A molecular orbital analysis of a model, Mo(HS)$_2$(HNC)$_4$, traces the deformation to the d^4 electron count. The lowest lying unoccupied MO consists of an S p–S p bonding combination and a Mo d orbital. The resulting imbalance in S–S bonding leads to an opening up of the S–Mo–S angle. The cyclic voltammogram shows two quasireversible redox events between −1.0 and +1.0 V, a one-electron reduction at $E_{1/2}$ = −0.17 V, and an oxidation at $E_{1/2}$ = +0.45 V. ^{1}H and ^{13}C NMR, UV–visible, and IR spectra are also reported.

While many six-coordinate d^4 metal complexes assume octahedral or near octahedral molecular structures,[2] significantly deformed octahedra have been found for Mo(II) compounds of the $MX_2L_2L'_2$ (X = monobasic anion such as Br^-, CH_3^-, RO^-; L, L' = neutral ligands such as pyridine, CO, PR_3) or M(S$_2$CNR$_2$)$_2$L$_2$ (L = CO) type.[3] We also know from the literature[4-6] that the Mo(II) ion seeks seven-coordination in its mononuclear complexes, thus achieving the inert-gas configuration. Examples may be found in Mo(RNC)$_7^{2+}$ and many mixed complexes containing CO and other ligands. Thus six-coordinate Mo(II) compounds are considered to be coordinatively unsaturated.

We have been interested in obtaining coordinatively unsaturated low-valent molybdenum compounds, possibly capable of binding biologically interesting substrates such as acetylene, CO, diazenes, or dinitrogen. Despite intensive current interest in (thiolato) metal complexes, the organosulfur ligands involved in low-valent molybdenum complexes so far have been rather limited. A vast chemistry of dithioacid and 1,1-dithiolate compounds containing Mo(IV) has developed,[7] but only a few monomeric Mo(II) or Mo(III) compounds are known, e.g., the above-mentioned carbonyldithiocarbamate Mo(II) compounds.[3b] This situation may be due to the strong propensity of Mo(II) or Mo(III) ion to form dimeric or polymeric compounds. Mononuclear, low-valent molybdenum compounds of monodentate thiolate are, to our best knowledge, completely absent in the literatures, apart from Mo(SR)$_2$(dppe)$_2$ (dppe = Ph$_2$PCH$_2$CH$_2$PPh$_2$).[8] Recently we were able to prepare a novel six-coordinate Mo(II) compound, Mo(*t*-BuS)$_2$(*t*-BuNC)$_4$[9a] (**1**) from Mo(*t*-BuS)$_4$.[9b] The deep emerald green compound **1** is diamagnetic. A general theoretical analysis of six-coordinate d^4 complexes[10] led us to anticipate a deformation in such a compound. A single-crystal X-ray diffraction study, described in this paper, indeed revealed a considerably deformed octahedron. The structural chemistry of the complex and a theoretical exploration of its deformation are the subject of this work. Compound **1** was found to be very substitution active and extremely versatile. The reaction chemistry, however, will be described elsewhere.

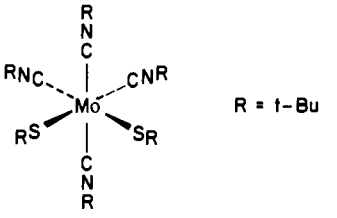

1

Experimental Section

Physical Measurements. Spectroscopic and electrochemical measurements were made by instruments described in the previous paper,[9a] in a pure nitrogen atmosphere. The ^{13}C NMR spectra were recorded on a JEOL 4H 100- or 360-MHz Bruker WM-360 wb instrument.

X-ray Crystallographic Procedure. A deep emerald green crystal (0.58 × 0.25 × 0.15 mm), grown from toluene-containing hexane (1:0.2 vol ratio), was carefully sealed in a Lindermann capillary under a nitrogen atmosphere and used for data collection.

Crystal data: $C_{28}H_{54}N_4S_2Mo$, M_r = 606.84, monoclinic, space group $P2_1/c$. On the basis of 48 reflections, the following unit cell parameters were obtained: a = 18.616 (7) Å, b = 11.823 (2) Å, c = 18.667 (6) Å, β = 116.00 (3)°, V(for Z = 4) = 3693 (2) Å^3, d_{calcd} = 1.09 g·cm^{-3}, and μ(Mo Kα) = 4.8 cm^{-1}.

Data were collected on an automated Philips PW1100 four-circle diffractometer with graphite-monochromated Mo Kα radiation (0.7107 Å). The diffracted intensities were measured by the ω–2θ technique with a take-off angle of 4.5°. The scan rate was 2°/min for 2θ. Background counts were taken at both ends of the scan range. A total of 4838

(1) (a) Department of Chemistry, Faculty of Engineering Science, Osaka University, Toyonaka, Osaka 560, Japan. (b) Department of Chemistry, Osaka City University, Sumiyoshiku, Osaka 558, Japan. (c) Department of Chemistry, Cornell University, Ithaca, NY, 14853.

(2) (a) Glavan, K. A.; Whittle, R.; Johnson, J. F.; Elder, R. C.; Deutsch, E. *J. Am. Chem. Soc.* **1980**, *102*, 2103-2104. (b) Bandoli, G.; Clemente, D. A.; Mazzi, U. *J. Chem. Soc., Dalton Trans.* **1976**, 125-130; *Ibid.* **1977**, 1837-1844. (c) Trop, H. S.; Davison, A.; Jones, A. G.; Davis, M. A.; Szalda, D. J.; Lippard, J. J. *Inorg. Chem.* **1980**, *19*, 1105-1117.

(3) (a) Chisholm, M. H.; Huffman, J. C.; Kelly, R. L. *J. Am. Chem. Soc.* **1979**, *101*, 7615-7617. (b) Templeton, J. L.; Ward, B. D. *Ibid.* **1980**, *102*, 6568-6569. (c) Drew, M. G. B.; Tomkins, I. B.; Colton, R. *Aust. J. Chem.* **1970**, *23*, 2517-2520.

(4) Stiefel, E. I. *Prog. Inorg. Chem.* **1977**, *22*, 1-223.

(5) (a) Lewis, D. F.; Lippard, S. J. *Inorg. Chem.* **1972**, *11*, 621-626. (b) Lewis, D. F.; Lippard, S. J. *J. Am. Chem. Soc.* **1975**, *97*, 2697-2702.

(6) (a) Wood, T. E.; Deaton, J. C.; Corning, J.; Wild, R. E.; Walton, R. A. *Inorg. Chem.* **1980**, *19*, 2614-2619 and references cited therein. (b) Chatt, J.; Pombeiro, A. J. L.; Richard, R. L. *J. Chem. Soc., Dalton Trans.* **1979**, *1585*-1590. (c) Brindon, B. J.; Edwards, D. A.; Paddick, K. E.; Drew, M. G. B. *Ibid.* **1980**, 1317-1323. (d) Girolami, G. S.; Andersen, R. A. *J. Organomet. Chem.* **1979**, *182*, C43-C45.

(7) Coucouvanis, D. *Prog. Inorg. Chem.* **1979**, *26*, 302-469.

(8) Chatt, J.; Lloyd, J. P.; Richard, R. L. *J. Chem. Soc., Dalton Trans.* **1976**, *565*-568.

(9) (a) Kamata, M.; Yoshida, T.; Otsuka, S.; Hirotsu, K.; Higuchi, T. *J. Am. Chem. Soc.* **1981**, *103*, 3572-4. (b) Otsuka, S.; Kamata, M.; Hirotsu, K.; Higuchi, T. *Ibid.* **1981**, *103*, 3011-4.

(10) Kubáček, P.; Hoffmann, R. *J. Am. Chem. Soc.* **1981**, *103*, 4320.

0002-7863/81/1503-5772$01.25/0

Table I. Fractional Coordinates and Temperature Factors for Mo(*t*-BuS)$_2$(*t*-BuNC)$_4$[a]

atom	*x*	*y*	*z*	*U*(11)	*U*(22)	*U*(33)	*U*(12)	*U*(13)	*U*(23)
Mo	0.26700 (4)	0.6508 (1)	0.21588 (4)	0.0425 (4)	0.0361 (4)	0.0397 (4)	−0.045 (4)	0.0222 (3)	−0.0008 (4)
S(1)	0.2437 (2)	0.8221 (2)	0.1427 (2)	0.063 (2)	0.049 (2)	0.071 (2)	0.001 (1)	0.038 (1)	0.015 (1)
S(2)	0.2691 (1)	0.4851 (2)	0.1452 (1)	0.045 (1)	0.046 (1)	0.059 (2)	0.000 (1)	0.024 (1)	−0.010 (1)
N(1)	0.0944 (5)	0.6249 (6)	0.2147 (5)	0.066 (5)	0.052 (5)	0.088 (6)	−0.004 (4)	0.050 (5)	0.002 (5)
N(2)	0.4446 (4)	0.7117 (7)	0.2378 (5)	0.047 (5)	0.080 (6)	0.068 (6)	−0.010 (5)	0.021 (4)	0.005 (5)
N(3)	0.3085 (6)	0.8123 (7)	0.3703 (5)	0.123 (8)	0.056 (6)	0.062 (6)	−0.005 (5)	0.052 (6)	−0.011 (4)
N(4)	0.3293 (6)	0.4875 (7)	0.3709 (5)	0.145 (9)	0.056 (6)	0.059 (6)	0.009 (6)	0.049 (6)	0.015 (5)
C(1)	0.1547 (5)	0.6338 (7)	0.2109 (5)	0.055 (6)	0.036 (5)	0.062 (6)	−0.007 (4)	0.037 (5)	0.002 (5)
C(2)	0.3810 (5)	0.6822 (7)	0.2287 (5)	0.048 (5)	0.044 (6)	0.046 (5)	−0.002 (4)	0.019 (4)	−0.001 (4)
C(3)	0.2931 (6)	0.7555 (8)	0.3149 (5)	0.077 (7)	0.048 (6)	0.055 (6)	−0.001 (5)	0.037 (6)	−0.002 (5)
C(4)	0.3072 (6)	0.5439 (8)	0.3155 (5)	0.082 (7)	0.046 (6)	0.048 (6)	−0.002 (5)	0.032 (5)	−0.000 (5)
C(5)	0.1410 (6)	0.8956 (8)	0.0971 (6)	0.071 (7)	0.049 (7)	0.087 (8)	0.017 (5)	0.036 (6)	0.021 (6)
C(6)	0.0816 (6)	0.7957 (10)	0.0416 (7)	0.057 (7)	0.090 (9)	0.107 (10)	0.006 (6)	0.023 (7)	0.012 (8)
C(7)	0.1479 (8)	0.9860 (10)	0.0475 (8)	0.119 (11)	0.068 (8)	0.139 (12)	0.022 (8)	0.066 (9)	0.060 (8)
C(8)	0.1190 (7)	0.9251 (10)	0.1632 (7)	0.114 (10)	0.076 (9)	0.126 (10)	0.027 (8)	0.086 (9)	−0.003 (8)
C(9)	0.1801 (5)	0.3930 (8)	0.1039 (5)	0.050 (6)	0.045 (6)	0.065 (7)	−0.003 (5)	0.020 (5)	−0.016 (5)
C(10)	0.1987 (6)	0.3001 (9)	0.0537 (7)	0.082 (8)	0.057 (7)	0.091 (8)	−0.001 (6)	0.036 (7)	−0.031 (6)
C(11)	0.1045 (6)	0.4615 (9)	0.0494 (6)	0.046 (6)	0.061 (7)	0.081 (8)	0.010 (5)	−0.002 (5)	−0.018 (6)
C(12)	0.1685 (7)	0.3358 (9)	0.1734 (7)	0.093 (8)	0.073 (8)	0.106 (9)	−0.014 (7)	0.062 (7)	0.007 (7)
C(13)	0.0275 (6)	0.6112 (10)	0.2335 (6)	0.058 (6)	0.098 (9)	0.094 (8)	−0.023 (6)	0.055 (6)	−0.023 (7)
C(14)	−0.0041 (9)	0.4925 (11)	0.2136 (10)	0.131 (12)	0.087 (10)	0.217 (17)	−0.036 (9)	0.122 (13)	−0.018 (11)
C(15)	−0.0400 (8)	0.6950 (14)	0.1738 (10)	0.073 (10)	0.153 (15)	0.195 (17)	0.025 (10)	0.042 (10)	0.004 (13)
C(16)	0.0483 (10)	0.6581 (17)	0.3121 (8)	0.148 (14)	0.289 (24)	0.092 (10)	−0.037 (15)	0.085 (10)	−0.046 (13)
C(17)	0.5149 (6)	0.7834 (10)	0.2585 (6)	0.049 (6)	0.091 (8)	0.058 (6)	−0.028 (6)	0.014 (5)	0.007 (6)
C(18)	0.5815 (7)	0.7080 (14)	0.2568 (10)	0.069 (9)	0.156 (15)	0.212 (17)	−0.004 (9)	0.077 (11)	−0.002 (13)
C(19)	0.4969 (8)	0.8761 (11)	0.1990 (8)	0.118 (11)	0.105 (11)	0.127 (11)	−0.018 (9)	0.040 (9)	0.065 (9)
C(20)	0.5387 (9)	0.8293 (14)	0.3428 (8)	0.134 (13)	0.213 (19)	0.100 (10)	−0.100 (13)	0.063 (10)	−0.067 (11)
C(21)	0.3167 (9)	0.8822 (10)	0.4370 (6)	0.202 (15)	0.086 (10)	0.040 (7)	0.037 (9)	0.028 (8)	−0.014 (6)
C(25)	0.3383 (10)	0.4183 (11)	0.4362 (7)	0.284 (19)	0.075 (9)	0.082 (9)	0.068 (11)	0.113 (11)	0.038 (8)

atom	*x*	*y*	*z*	*U*, Å^2	atom	*x*	*y*	*z*	*U*, Å^2
C(22)	0.2427 (15)	0.8423 (20)	0.4591 (15)	0.244 (11)	C(26)	0.3904 (10)	0.4713 (15)	0.5143 (10)	0.157 (6)
C(23)	0.3087 (15)	0.9993 (22)	0.4064 (15)	0.251 (11)	C(27)	0.3588 (12)	0.3018 (17)	0.4245 (12)	0.185 (8)
C(24)	0.3997 (16)	0.8583 (21)	0.5186 (16)	0.258 (12)	C(28)	0.2535 (21)	0.4170 (26)	0.4376 (20)	0.333 (16)

[a] Standard deviations of the least significant figures are given in parentheses.

reflections were obtained for a 2θ range of 2.0–46.0°, of which 3355 have $I > 3\sigma(I)$ and were considered as observed. Three reference reflections monitored every 180 min displayed neither systematic nor significant deviations from their initial intensities. The intensities were corrected for Lorentz and polarization factors, but no absorption correction was applied.

The structure was solved by MULTAN.[11] From the *E* map, molybdenum and two sulfur atoms were located. The remaining non-hydrogen atoms were located in succeeding difference Fourier syntheses. The structure was refined by least-squares techniques, minimizing the function $\sum w(|F_o| - |F_c|)^2$; the weights were assigned as $1.0/\sigma(F_o)^2$. R and R_w were 0.098 and 0.115 after three cycles of isotropic refinement. In the following refinement, anisotropic temperature factors were assigned to the Mo, S, N, and 22 of the 28 carbon atoms. Isotropic temperature factors were assigned to the other six carbon atoms, since previous least-squares calculation indicated very large thermal motion of these atoms. Final least-squares refinement converged to $R = 0.069$ and $R_w = 0.086$.[12] Neutral atomic scattering factors of Cromer and Waber[13] were used for all atoms. They were all corrected for the real part of the anomalous dispersion. Fractional coordinates and thermal parameters are listed in Table I. The bond lengths and bond angles are shown in Tables II and III, respectively. The equatorial plane 1 is defined as the least-squares plane containing two S atoms and two carbon atoms, C(3) and C(4). Selected dihedral angles are shown in Table IV. The important intermolecular distances are listed in Table V. A table of structure factors is available as supplementary material to this paper.

Table II. Bond Distances (Å) of Mo(*t*-BuS)$_2$(*t*-BuNC)$_4$[a]

Mo-S(1)	2.374 (3)	C(5)-C(7)	1.545 (18)
Mo-S(2)	2.372 (3)	C(5)-C(8)	1.532 (20)
Mo-C(1)	2.061 (10)	C(9)-C(10)	1.578 (16)
Mo-C(2)	2.062 (10)	C(9)-C(11)	1.555 (12)
Mo-C(3)	2.097 (10)	C(9)-C(12)	1.559 (18)
Mo-C(4)	2.097 (9)	C(13)-C(14)	1.504 (17)
S(1)-C(5)	1.875 (10)	C(13)-C(15)	1.604 (17)
S(2)-C(9)	1.846 (9)	C(13)-C(16)	1.453 (20)
N(1)-C(1)	1.160 (14)	C(17)-C(18)	1.538 (20)
N(1)-C(13)	1.444 (16)	C(17)-C(19)	1.490 (18)
N(2)-C(2)	1.174 (13)	C(17)-C(20)	1.535 (18)
N(2)-C(17)	1.462 (13)	C(21)-C(22)	1.669 (37)
N(3)-C(3)	1.159 (13)	C(21)-C(23)	1.480 (28)
N(3)-C(21)	1.446 (15)	C(21)-C(24)	1.650 (25)
N(4)-C(4)	1.143 (12)	C(25)-C(26)	1.490 (19)
N(4)-C(25)	1.417 (17)	C(25)-C(27)	1.471 (25)
C(5)-C(6)	1.557 (14)	C(25)-C(28)	1.590 (47)

[a] Standard deviations of the least significant figure of each distance are given in parentheses.

Results and Discussion

Physical Properties. The title compound, **1**, which can be obtained selectively from reaction of Mo(*t*-BuS)$_4$ with an excess of *t*-BuNC,[9a] is thermally fairly stable. After the toluene solution was heated at 100 °C for 10 h, it can be recovered without substantial loss. In the solid state it is moderately stable to air but in solution it reacts immediately with dioxygen. Compound **1** is soluble in most organic solvents, even slightly soluble in saturated hydrocarbons. It readily forms a well-developed single crystal suitable for X-ray crystallography.

The electronic spectrum of **1** in hexane (Table VI) is characterized by a very intense charge-transfer band at 33 700 cm^{-1} and several other strong absorptions in visible region. The IR CN stretching vibrations of the Nujol-mulled sample appear at 2120, 2080 (sh), and 1997 cm^{-1} and those of the hexane solution at 2120 (sh) and 2010 cm^{-1}. These values may be compared with those of Mo(*t*-BuNC)$_7^{2+}$[4,5] and Mo(MeNC)$_7^{2+}$,[14] which fall in the range of 2140–2160 cm^{-1}. The lower frequencies of **1**, showing the electron-donating effect of the thiolate ligands, are reasonable.

(11) Germain, G.; Main, P.; Woolfson, M. M. *Acta Crystallogr., Sect. B* **1970**, *B26*, 274–285. Woolfson, M. M. *Acta Crystallogr., Sect. A* **1977**, *A33*, 219–225.

(12) Sakurai, T., Ed. "Unics, The Universal Crystallographic Computation Program System", The Crystallographic Society of Japan, 1967. Johnson, C. K. "ORTEP", Oak Ridge National Laboratory Report ORNL-TM-3794.

(13) Cromer, D. T.; Waber, J. T. "International Tables for X-ray Crystallography"; Ibers, J. A.; Hamilton, W. C., Eds.; Kynoch Press: Birmingham, England, 1974; Vol. IV, Table 2.2A, p 72.

Table III. Bond Angles (Deg) in Mo(*t*-BuS)$_2$(*t*-BuNC)$_4$[a]

S(1)-Mo-S(2)	115.3 (1)	C(10)-C(9)-C(11)	110.2 (7)
S(1)-Mo-C(1)	97.5 (2)	C(10)-C(9)-C(12)	109.8 (8)
S(1)-Mo-C(2)	80.4 (2)	C(11)-C(9)-C(12)	110.8 (9)
S(1)-Mo-C(3)	85.3 (3)	N(1)-C(13)-C(14)	109.3 (11)
S(1)-Mo-C(4)	158.2 (2)	N(1)-C(13)-C(15)	105.0 (11)
S(2)-Mo-C(1)	99.1 (2)	N(1)-C(13)-C(16)	109.0 (10)
S(2)-Mo-C(2)	86.9 (3)	C(14)-C(13)-C(15)	107.6 (9)
S(2)-Mo-C(3)	157.5 (2)	C(14)-C(13)-C(16)	120.5 (14)
S(2)-Mo-C(4)	84.8 (3)	C(15)-C(13)-C(16)	104.3 (12)
C(1)-Mo-C(2)	174.0 (3)	N(2)-C(17)-C(18)	107.1 (10)
C(1)-Mo-C(3)	86.3 (4)	N(2)-C(17)-C(19)	110.3 (8)
C(1)-Mo-C(4)	86.7 (4)	N(2)-C(17)-C(20)	107.4 (11)
C(2)-Mo-C(3)	87.8 (4)	C(18)-C(17)-C(19)	109.4 (12)
C(2)-Mo-C(4)	93.2 (4)	C(18)-C(17)-C(20)	110.7 (10)
C(3)-Mo-C(4)	73.7 (4)	C(19)-C(17)-C(20)	111.9 (11)
Mo-S(1)-C(5)	119.7 (4)	N(3)-C(21)-C(22)	105.3 (12)
Mo-S(2)-C(9)	119.2 (4)	N(3)-C(21)-C(23)	104.3 (14)
C(1)-N(1)-C(13)	170.5 (9)	N(3)-C(21)-C(24)	113.5 (15)
C(2)-N(2)-C(17)	160.2 (10)	C(22)-C(21)-C(23)	114.0 (17)
C(3)-N(3)-C(21)	172.4 (13)	C(22)-C(21)-C(24)	105.3 (16)
C(4)-N(4)-C(25)	166.9 (14)	C(23)-C(21)-C(24)	114.3 (14)
Mo-C(1)-N(1)	174.4 (8)	N(4)-C(25)-C(26)	112.3 (12)
Mo-C(2)-N(2)	172.8 (8)	N(4)-C(25)-C(27)	110.7 (15)
Mo-C(3)-N(3)	179.0 (8)	N(4)-C(25)-C(28)	106.1 (15)
Mo-C(4)-N(4)	178.6 (8)	C(26)-C(25)-C(27)	116.0 (13)
S(1)-C(5)-C(6)	108.3 (7)	C(26)-C(25)-C(28)	102.3 (18)
S(1)-C(5)-C(7)	104.1 (8)	C(27)-C(25)-C(28)	108.5 (17)
S(1)-C(5)-C(8)	109.6 (7)		
C(6)-C(5)-C(7)	110.3 (9)		
C(6)-C(5)-C(8)	112.5 (10)		
C(7)-C(5)-C(8)	111.8 (9)		
S(2)-C(9)-C(10)	105.5 (7)		
S(2)-C(9)-C(11)	110.8 (6)		
S(2)-C(9)-C(12)	109.6 (6)		

[a] The standard deviation of the least significant figure of each angle is given in parentheses.

Table IV. The Least-Squares Plane 1 and Selected Dihedral Angles in Mo(*t*-BuS)$_2$(*t*-BuNC)$_4$

(a) Displacement (Å) of Atoms from the Least-Squares Plane 1

plane 1: S(1), S(2), C(3), C(4)

S(1) −0.007 (4), S(2) 0.007 (4), C(3) 0.011 (6), C(4) −0.011 (6), Mo −0.142 (4), N(1) −3.300 (10), N(2) 3.055 (9), N(3) 0.11 (1), N(4) 0.06 (2), C(1) −2.18 (1), C(2) 1.91 (1), C(5) −1.58 (1), C(9) −1.54 (1)

(b) Definitions of Other Planes

plane 2: S(1), Mo, S(2)
plane 3: C(3), Mo, C(4)
plane 4: Mo, S(1), C(5)
plane 5: Mo, S(2), C(9)
plane 6: C(1), Mo, C(2)

(c) Selected Dihedral Angles

plane 1-plane 4	86 (1)°	plane 1-plane 6	83 (1)°
plane 1-plane 5	84 (1)°	plane 2-plane 3	11 (1)°

Table V. Intermolecular Distances Less Than 4.0 Å in Mo(*t*-BuS)$_2$(*t*-BuNC)$_4$[g]

C(7)-C(10)[a]	3.82 (2)	C(20)-S(2)[d]	3.94 (2)
C(23)-C(27)[a]	3.67 (3)	C(28)-C(20)[e]	3.78 (4)
C(10)-C(15)[b]	3.97 (2)	C(22)-S(1)[f]	3.93 (3)
C(11)-C(11)[b]	3.62 (2)	C(22)-S(2)[f]	3.87 (3)
C(8)-C(14)[c]	3.85 (3)	C(24)-N(2)[f]	3.89 (3)
C(15)-C(14)[c]	3.99 (2)	C(26)-C(19)[f]	3.62 (2)
		C(28)-C(7)[f]	3.60 (5)

[a-f] The symmetry transformations of the second atom are as follows: (*a*) $x, 1+y, z$; (*b*) $-x, 1-y, -z$; (*c*) $-x, {}^1/_2+y, {}^1/_2-z$; (*d*) $1-x, {}^1/_2+y, {}^1/_2-z$; (*e*) $x, {}^1/_2-y, {}^1/_2+z$; (*f*) $x, {}^3/_2-y, {}^1/_2+z$. [g] The standard deviation of the least significant figure of each distance is given in parentheses.

The ^{1}H NMR shows only one sharp singlet resonance for the *t*-BuNC ligands, whereas the ^{13}C NMR gives at ambient temperature a pair of singlet signals for methyl and tertiary carbon atoms of *t*-BuNC, as indicated in Table VI. The ^{13}C signals of the isocyanide carbon atoms coordinated to the metal were not observed, presumably due to the nuclear Overhauser effect.

Table VI. Selected Spectral Data of Mo(*t*-BuS)$_2$(*t*-BuNC)$_4$

UV-Visible in Hexane				
λ_{max}, nm	297	425	450 sh	690
ϵ	30000	6000	4800	680
IR, cm^{-1} (Nujol mull)				
$\nu_{N\equiv C}$	2120 s	2080 s	1997 vs	
other bands[a]	433 sh	420 s	400 w	372 m
	345 w	332 w	318 m	305 m

^{1}H NMR in C_6D_6,[b] δ(Me_4Si)

$(CH_3)_3CNC$ 1.23 (s) $(CH_3)_3CS$ 1.98 (s)

^{13}C NMR in Toluene-d_8-Et_2O,[c] ppm

	27 °C	−100 °C
$(CH_3)_3CNC$	31.17, 31.76	30.56, 31.08
$(CH_3)_3CNC$	55.03, 57.62	54.49, 56.60
$(CH_3)_3CS$	35.80	36.12 (31 Hz)[d]
$(CH_3)_3CS$	48.22	48.28

[a] Listed are only low-frequency bands appearing in the metal-ligand vibrational region. [b] Measured at 27 °C. [c] Measured by a 100-MHz instrument. [d] Half-height width.

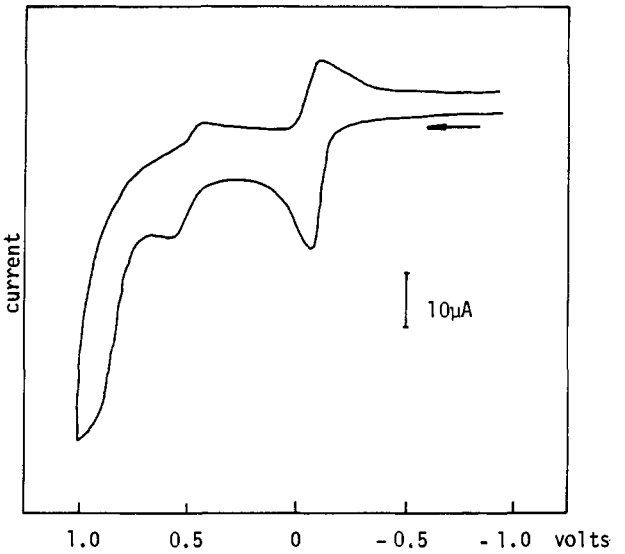

Figure 1. Cyclic voltammogram of Mo(*t*-BuS)$_2$(*t*-BuNC)$_4$ in DMF-Et_4NClO_4 (scan rate 100 mV s^{-1}; potential vs. SCE).

The temperature dependence of the ^{13}C NMR spectrum of **1** was studied in a toluene-d_8–diethyl ether mixture. The methyl carbon signals of both *t*-BuNC (two singlets) and *t*-BuS ligands (one singlet) broaden at low temperature (−70 to 100 °C) while the tert carbon signals remain as sharp singlets even at −100 °C (Table VI). The low-temperature spectrum shows no indication of appearance of new signals. The broadening indicates a hindered rotation of the methyl groups of *t*-BuNC and *t*-BuS ligands at low temperature. The same spectral features were obtained with a 360-MHz NMR instrument.

The electrochemical properties of **1** in DMF were studied by cyclic voltammetry. The cyclic voltammogram is shown in Figure 1. Two redox events are observable between −1.0 and +1.0 V (vs. SCE). With sweep rates between 100 and 200 mV/s, $i_{p,a}/i_{p,c} \simeq 1$ and $i_p/v^{1/2}$ was constant for both reduction and oxidation waves. The potential difference between the anodic and cathodic wave peaks ΔE_p was in the range of 70–100 mV and increased slightly with an increase in sweep rate. Thus the two redox processes clearly are quasi-reversible, the reduction at $E_{1/2} = -0.17$ V and oxidation at $E_{1/2} = +0.45$ V (vs. SCE). For the mixed Mo(II) complex, $[Mo(RNC)_{7-x}(PR'_3)_x]^{2+}$ ($x = 1, 2$), only an oxidation wave in the cyclic voltammogram was observed and the $E_{1/2}$ values were in a range of +0.90 to +1.18 V.[6a] The lower oxidation potential of the neutral complex **1**, compared to the cationic mixed Mo(II) compounds, appears to be reasonable. With the capability

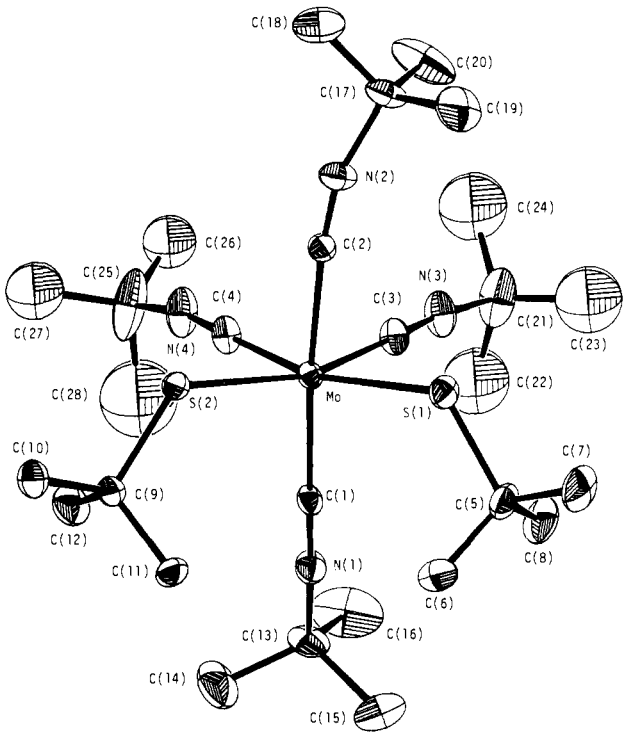

Figure 2. Perspective view of a molecule of $Mo(t\text{-}BuS)_2(t\text{-}BuNC)_4$.

of alkylthiolato ligands to stabilize higher oxidation states of a metal center being greater than that of tertiary phosphines, this effect may also be operating.

Description of the Crystal Structure. The geometry of the complex is illustrated together with the numbering scheme in Figure 2. Figure 3 shows a stereoview of the molecular packing in the unit cell. The six-coordinated molecule as a whole has no symmetry element, the closest symmetry point group for the MoS_2C_4 fragment being C_{2v}.

The most conspicuous feature of the structure is the wide SMoS angle of 115.3°. Accordingly the angles C(3)MoC(4), S(1)-MoC(3), and S(2)MoC(4) become smaller than 90° (Table III). The nonbonded S(1)–S(2) distance is 4.010 (3) Å which is longer than the sum (3.70 Å) of van der Waals radius of divalent S atom. The four equatorial atoms S(1), S(2), C(3), and C(4) deviate only slightly from their least-squares plane 1 (Table IV). The Mo atom lies 0.146 Å below this plane and toward C(1). Note that angles S(1)MoC(1) and S(2)MoC(1) are slightly greater than 90°. A noncrystallographic symmetry plane bisecting the S(1)MoS(2) angle and perpendicular to plane 1 nearly bisects the C(3)MoC(4) angle. However, the C(1) and C(2) atoms are slightly displaced from this symmetry plane. Furthermore, the two axial bonds, MoC(1) and MoC(2), are bent forward, making angles 81 and 83° with plane 1, respectively. The deviations of the two axial isocyanide ligands from the *y* axis perpendicular to plane 1 are illustrated in Figure 4, which shows a projection on plane 1 of the isocyanide atoms C(1)N(1)C(13) and C(2)N(2)C(17).

Another notable feature of the structure may be the syn alignment of the two S–C bonds. The two angles MoS(1)C(5) and MoS(2)C(9) are nearly the same (119.7 and 119.2°). The planes MoS(1)C(5) and MoS(2)C(9), which define the direction of the sulfur lone pair orbitals, form with plane 1 angles 86 and 84°, respectively. Thus the perpendiculars to these planes lie approximately in plane 1. Since the molecule contains six bulky *tert*-butyl groups, their intramolecular nonbonded contacts deserve scrutiny. The closest C–C distance between two thiolate *tert*-butyl groups is 3.97 Å (C(6)–C(11)), and all other nonbonded C–C distances between *tert*-butyl groups of *t*-BuS and *t*-BuNC are 4.05 Å (C(12)–C(14)) or more, implying that the present molecular geometry is not due to the steric effect of *tert*-butyl groups.

The bond distance of the axial isocyanide carbon to the Mo(II) atom is a little shorter (~0.035 Å) than that of the equatorial one. We could not, however, find significant differences in geometry around the C≡N moieties between the axial and equatorial isocyanide ligands, their C≡N distances and C≡N—C angles being nearly the same, within the experimental errors, except for the C(2)—N(2)—C(17) angle.

Comparison with Related Compounds. Only a few mononuclear Mo(II) compounds have been studied by X-ray crystallography, $Mo(RNC)_7^{2+}$,[5,14] $Mo(RNC)_6X^+$,[15] $Mo(t\text{-}BuO)_2(py)_2(CO)_2$,[16] $Mo[S_2CN(i\text{-}Pr)_2]_2(CO)_2$,[3b] and $MoBr_2(CO)(PPh_3)_2$.[3c] The Mo–S bond distance (2.37 Å) of $Mo(t\text{-}BuS)_2(t\text{-}BuNC)_4$ seems to be reasonable in comparison with 2.235 Å for the tetracoordinate Mo(IV) compound, $Mo(t\text{-}BuS)_4$. The mercapto sulfur–Mo(IV) distance in the six-coordinate Mo(IV) compound, $Mo(SCH_2CH_2SCH_2CH_2S)_2$,[17] is 2.36 Å (average). The distance of 2.37 Å in our complex appears to be short for a six-coordinate Mo(II) compound. It may be reflecting the effect of d_π-accepting alkylisocyanide ligands.

The Mo(II)–C(isocyanide) distances in seven-coordinate Mo(II) compounds are 2.05–2.14 Å for $Mo(t\text{-}BuNC)_7^{2+}$,[5b] 2.04–2.16 Å for $Mo(CH_3NC)_7^{2+}$,[14] and 2.05–2.12 Å for $Mo(t\text{-}BuNC)_8Br^+$.[15] The distances 2.06 and 2.10 Å found for **1** are comparable to those of the above seven coordinate complexes. From the smaller coordination number, a shorter distance would have been expected.[18] The observed Mo(II)–S bond distance could then be ascribed to two competing factors, the electron-donating effect from the two thiolate ligands and the decrease in coordination number.

The electron transfer to the isocyanide ligand through d_π–p_π bonding should be reflected in the geometry, in particular the C≡N distance and C≡N—C angle. The available X-ray diffraction data are not accurate enough to discern any meaningful difference in the C≡N distance. The C≡N—C angle is more sensitive. In fact, the angle found for $Mo(CH_3NC)_7^{2+}$, $Mo(t\text{-}BuNC)_7^{2+}$, and $Mo(t\text{-}BuNC)_6Br^+$ are much closer to 180° than in the present compound (Table III), a feature consistent with the Mo(II)-C bond distances discussed above. A caution may be necessary here. We observe a distinctly small C≡N—C angle of 160° for one of the axial ligands whose C≡N– and Mo-C(2) vectors deviate considerably from the *y* axis. This is partly due to crystal packing, as is apparent from the close nonbonding contacts between the axial and the equatorial *tert*-butyl groups of adjacent molecules (see Figures 2 and 3 and Table V).

Molecular Orbital Analyses of the Structure. The orientation of *t*-Bu substituents of the thiolate ligands and the substantial distortion from the ideal octahedral structure: a larger S–Mo–S angle and a concomitant smaller C–Mo–C angle in the equatorial plane—these are structural features characteristic to $Mo(t\text{-}BuS)_2(t\text{-}BuNC)_4$. The bulk of the *t*-Bu substituents appears to have no direct correlation with the observed geometrical features. Then why does the molecule choose the structure that it possesses? In an attempt to answer this question, we have carried out molecular orbital calculations on the simplified model compound $Mo(HS)_2(HNC)_4$.

First compare the total energies computed for the four extreme orientations of the SH groups in $Mo(HS)_2(HNC)_4$. The relative energies are given below in **2**–**5**, assuming a low-spin d^4 configuration. At this point we employ the idealized octahedral arrangement of ligands at Mo, which will be a convenient reference point for our study of the distortion. The model isocyanide ligand (CNH) is assumed linear and the Mo–S–H angle is fixed to be 120°. The "syn-upright" orientation **2**, which is the observed conformation of $Mo(t\text{-}BuS)_2(t\text{-}BuNC)_4$, was calculated to be most stable among the four. The "anti-upright" conformer **3** is as stable as **2**, while the two "in-plane" conformers **4** and **5** are less stable

(14) Brant, P.; Cotton, F. A.; Sekutowski, J. C.; Wood, T. E.; Walton, R. A. *J. Am. Chem. Soc.* **1979**, *101*, 6588–6593.
(15) Lam, C. T.; Novotny, M.; Lewis, D. L.; Lippard, S. J. *Inorg. Chem.* **1978**, *17*, 2127–2133.
(16) See reference 3a.
(17) Hyde, J.; Magin, L.; Zubieta, J. *J. Chem. Soc., Chem. Commun.* **1980**, 204–205.
(18) (a) Mason, R. *Chem. Soc. Rev.* **1972**, *1*, 431–444. (b) Otsuka, S.; Yoshida, T.; Matsumoto, M.; Nakatsu, K. *J. Am. Chem. Soc.* **1976**, *98*, 5850–5858.

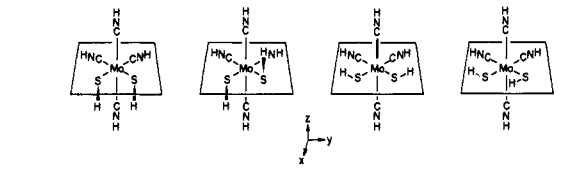

2 3 4 5

than **2** by 14.6 and 15.5 kcal/mol, respectively.

The frontier molecular orbitals (MO's) of each conformation are compared in Figure 5. These levels comprise primarily Mo d orbitals. The "e_g–t_{2g}" splitting pattern of the octahedral symmetry is basically retained so that three d_π orbitals (xz, yz, x^2-y^2) stay at low and two d_σ orbitals (z^2, xy) are high lying. The most striking aspect of the level scheme is that the "t_{2g}" set of conformers **2** and **3** splits further in a "two below one" manner. The two lowest levels, xz and yz, accept four electrons and the upper level, x^2-y^2, remains unoccupied. The presence of a low-lying vacant orbital is consistent with the small reduction potential, $E_{1/2} = -0.17$ eV, observed for Mo(t-BuS)$_2$(t-BuNC)$_4$. The HOMO–LUMO energy gap was calculated to be 0.63 eV for either **2** or **3**. In contrast the t_{2g} orbitals of **4** and **5** remain nearby triply degenerate at around the original Mo 4d energy, −11.06 eV. The lowering of the xz and yz levels is the reason that the conformations **2** and **3** are more stable than **4** and **5**.

An analysis of the orbital patterns of Figure 5 is not difficult. Since the t_{2g} set is involved in π bonding, our discussion must focus on the π-bonding capability of the isocyanide and thiolato ligands. The RNC group is both a π donor, through **6**, and a π acceptor, through **7**. One presumes, and our calculations concur, that the acceptor characteristics of the isocyanide dominate.

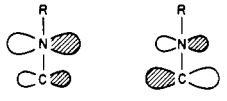

6 **7**

The thiolato or mercaptide ligand is a donor (if we neglect d orbitals on S, as we think one should) through two nonequivalent lone pairs. The better donor is the higher lying pure 3p lone pair orthogonal to the M–S–R plane and is shown in two orientations in **8a** and **8b**. The poorer donor is the lower lying σ lone pair in the M–S–R plane, **9a** and **9b**.

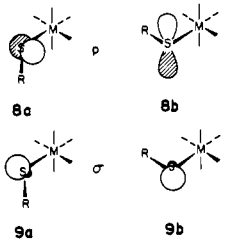

8a **8b**

9a **9b**

We illustrate the t_{2g} orbitals of **2** (syn upright) and **4** (in-plane I) in **10**. The corresponding orbital pictures for **3** (anti upright) and **5** (in plane II) are very similar to those for **2** and **4**, respectively. As may be seen in **10**, the level ordering in the t_{2g} set is a consequence of a different magnitude of bonding and antibonding interactions between Mo d_π and ligand orbitals: π and π^* of CNH; p and σ (lone pair) of SH. In any of molecular orbitals drawn in **10**, Mo d_π interacts with carbon p_π of CNH always in a bonding manner. Strictly speaking the phase relationship is the net outcome of a three-way mixing between d(Mo), π and π^*(CNH), orbitals where, in this case, the d–π^* bonding interaction appears to dominate over the others. Second-order perturbation arguments[19] would put this situation on a firmer

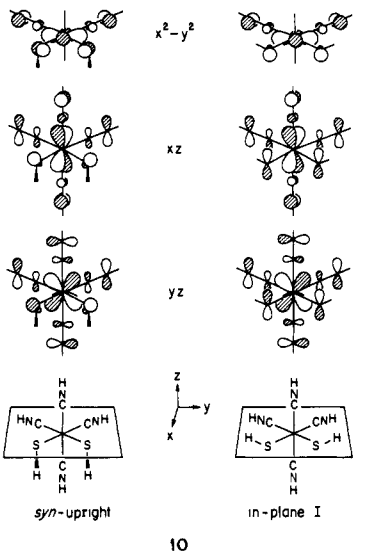

10

theoretical basis. The in-phase relationship accords with the chemical intuition that isocyanide ligands act as π acceptors. On the other hand, the Mo–S interaction is always antibonding, no matter which of the sulfur orbitals, p or (σ), is used. Of these the Mo d_π–S p antibonding interaction is the most significant.

For the "upright" geometries both xz and yz are stabilized because five d_π–π^*(CNH) attractive interactions overwhelm two d_π–σ(S) repulsive interactions. The destabilization of the x^2-y^2 is due to the strong d_π–p(S) repulsion. For the in-plane geometries, the bonding and antibonding contributions balance quite well: five attractive d_π–π^*(CNH) vs. two repulsive d_π–p(S) for the xz and yz, two attractive d_π–π^*(CNH) vs. two repulsive d_π–σ(S) for the x^2-y^2. Thus the near triple degeneracy of the three d_π orbitals is an accidental one.

Although the observed solid-state geometry of Mo(t-BuS)$_2$(t-BuNC)$_4$ shows only the "syn-upright" **2** conformation, the "anti-upright" **3** one is also a possibility. There are two plausible pathways for isomerization, proceeding through intermediate geometries **11a** and **11b**. For the Mo(HS)$_2$(HNC)$_4$ model the

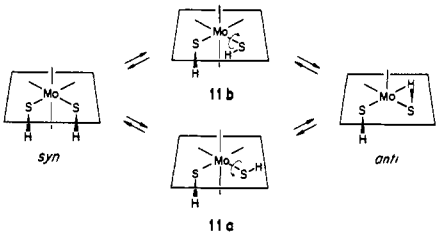

calculated energy barriers to the two kinds of rotation amount to 6.4 kcal/mol (**11a**) and 7.2 kcal/mol (**11b**). The ^{13}C NMR spectrum of Mo(t-BuS)$_2$(t-BuNC)$_4$ (**1**) in solution at ambient temperature shows a pair of singlet signals for both methyl and *tert*-butyl carbon atoms of t-BuNC. At low temperature (−100 °C) only broadening of the methyl signals is observed, while the *tert*-butyl carbon signals remain as sharp singlets. If the solid-state structure, syn upright, is retained in solution, three magnetically inequivalent *tert*-butyl carbon signals would be expected. Various reasons for a contrary observation are conceivable, e.g.: (1) in the syn-upright conformation **2**, the orientation of *tert*-butyl groups of two t-BuS ligands does not create a significant magnetic asymmetry for the two axial isocyanide carbons, (2) the *tert*-butyl carbon signals of the two conformers, **2** and **3**, are accidentally degenerate, (3) the energy barrier for the conformational exchange between **2** and **3** is very low, perhaps less than a few kilocalories per mole, (4) the molecule in solution has the anti-upright geometry **3**. Our approximate MO calculations on a simplified model do not have anything to say about the first two alternatives. They do not rule out 3, but it must be said that we would have thought the real molecule to have a larger rotational barrier than the model.

(19) See for instance: Libit, L.; Hoffmann, R. *J. Am. Chem. Soc.* **1974**, *96*, 1370–1383. The shape of the CN contribution in **10** is the outcome of such polarization.

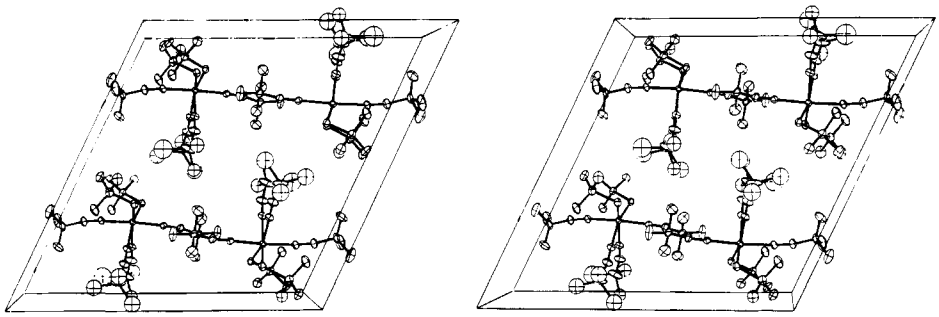

Figure 3. Stereoview of the unit cell contents of Mo(*t*-BuS)$_2$(*t*-BuNC)$_4$.

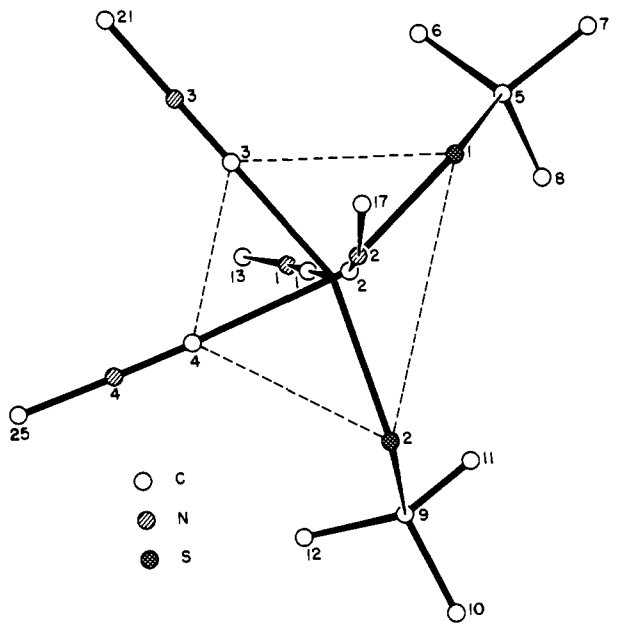

Figure 4. Projection of a molecule of Mo(*t*-BuS)$_2$(*t*-BuNC)$_4$ on the plane(1), some terminal groups being omitted.

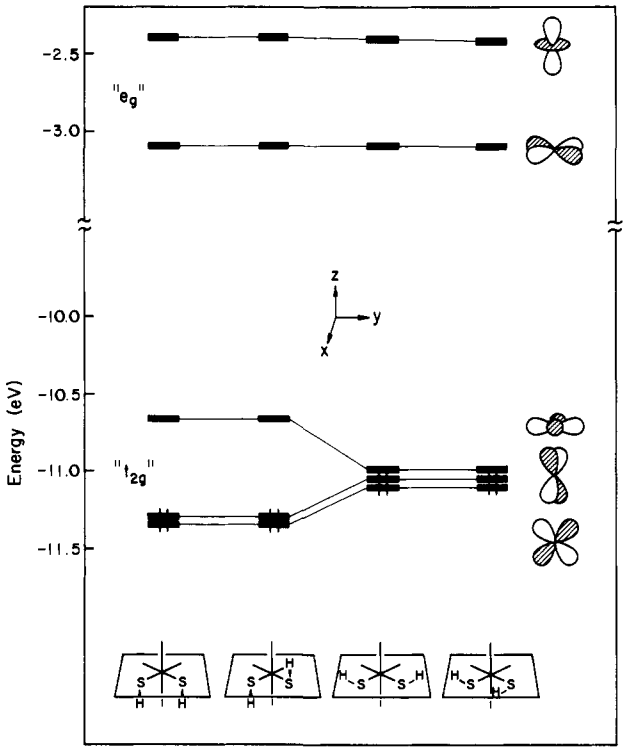

Figure 5. d orbital energy levels calculated for the four extreme orientations of the SH groups in Mo(HS)$_2$(HNC)$_4$.

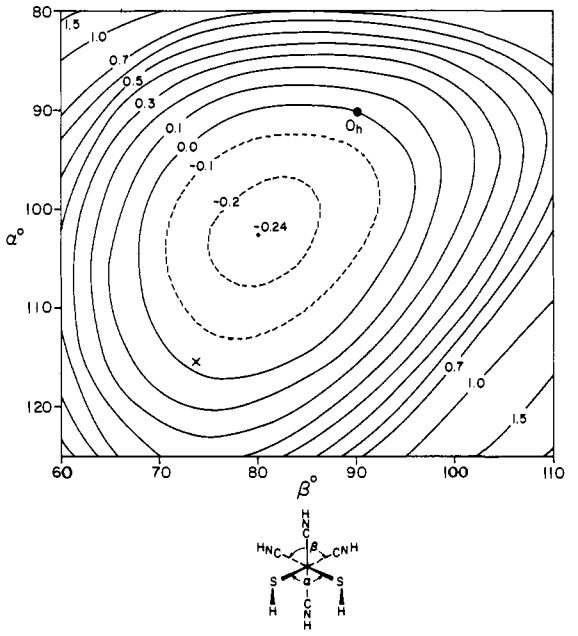

Figure 6. Potential energy surface for the deformation of syn-upright Mo(HS)$_2$(HNC)$_4$. The contours are in electronvolt relative to an energy zero at the idealized octahedral geometry (O_h), $\alpha = \beta = 90°$. The point marked by X indicates the experimentally observed structure of Mo(*t*-BuS)$_2$(*t*-BuNC)$_4$.

Now we allow the model compound Mo(HS)$_2$(HNC)$_4$ to distort from the ideal octahedral geometry. The variational parameters chosen are S–Mo–S angle α and C–Mo–C angle β in the equatorial plane, as shown in **12**. The orientation of the two SH groups

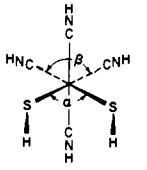

12

is the "syn-upright" one, and the axial CNH ligands are kept undistorted. Figure 6 shows the computed potential surface as a function of α and β. Obviously the octahedral geometry is not the most stable one. Instead the S–Mo–S angle tends to open up from 90°, while the C–Mo–C angle tends to decrease from 90°. The calculated surface reproduces qualitatively the way that Mo(*t*-BuS)$_2$(*t*-BuNC)$_4$ deforms. In the rather soft surface, a potential minimum is found at $\alpha \simeq 102.5°$ and $\beta \simeq 80.0°$. The observed angles of Mo(*t*-BuS)$_2$(*t*-BuNC)$_4$ are $\alpha = 115.3°$ and $\beta = 73.7°$. Given the approximate nature of our calculations, especially the lack of bulky *t*-Bu substituents, we are not unhappy with the discrepancy between the theoretical and experimental numbers.

We have also calculated the potential surface for the model with two extra electrons, i.e., d^6 Mo(HS)$_2$(HNC)$_4^{2-}$. A potential minimum was found at the ideal octahedral geometry, $\alpha = \beta = 90°$. The d^4 electron count is therefore essential for substantial

distortion, and it is not merely the bulk of the SR ligands that somehow "pushes them apart". The effect is more subtle.

There is a temptation here to rationalize the distortion in terms of Jahn–Teller arguments, because three low-lying orbitals t_{2g} compete with each other for four electrons. The following orbital analysis, however, shows that the real reason is not the Jahn–Teller effect but something else.

Orbital diagram **13** shows how the t_{2g} energy levels vary from

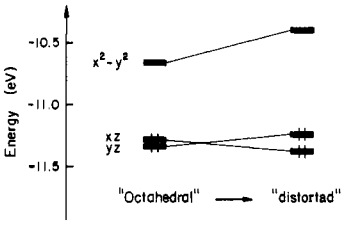

13

the octahedral ($\alpha = \beta = 90°$) to the distorted geometry ($\alpha = 102.5°$, $\beta = 80.0°$). The two occupied levels change their energy, but only very slightly. Furthermore stabilization of xz and destabilization of the yz offset each other. Thus the origin of the distortion cannot be attributed to these d orbitals. The unoccupied $x^2 - y^2$ level moves up, increasing the HOMO–LUMO energy gap from 0.63 to 0.84 eV. The number increases even further to 1.04 eV, when we take the observed angles, $\alpha = 115.3°$ and $\beta = 73.7°$. Although the energy gap is not very large, we think our calculations reflect the observed diamagnetism of Mo(t-BuS)$_2$(t-BuNC)$_4$.

Now we know that the occupied xz and yz are not responsible for the distortion. We find instead that the stabilization comes primarily from the second orbital below the HOMO **14**, which

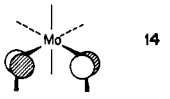

14

is made up from an out-of-phase combination of the two S p orbitals. The symmetry (strictly speaking pseudosymmetry) of the problem does not allow any substantial mixing of an Mo orbital into **14**. The distortion stabilizes **14** by –0.25 eV owing to a relief of the S p–S p repulsive interaction. This *is* a steric rationale. Then why is the d^4 electron count important? While the antibonding combination of the S p orbitals is well isolated in **14**, their bonding combination is spread out over several occupied levels and *also in the unoccupied* $x^2 - y^2$, which may be seen in the orbital picture **10**. For the d^4 molecule the antibonding contribution prevails over the bonding counterpart, which results in an opening up of the S–Mo–S angle. In contrast, the population of the $x^2 - y^2$ by two electrons cancels the dominant role of the antibonding interaction and allows the molecule to reveal stereochemical rigidity as a typical d^6 octahedral system. The interligand interaction between the two CNH groups appears to be of no importance in this particular molecule. The C–Mo–C angle is decreased in order to avoid the steric problem which is caused by the larger S–Mo–S angle.

A crystal structure of the d^8 planar complex *cis*-Pt(HS)$_2$(Ph$_3$P)$_2$ has recently been reported.[20] In light of the d^8 (square planar)–d^6 (octahedral) analogy, the electronic structure of the platinum complex corresponds to that of Mo(t-BuS)$_2$(t-buNC)$_4$ with two more electrons, thus a d^6 electron count. The observed deformation of *cis*-Pt(HS)$_2$(Ph$_3$P)$_2$ from an idealized square-planar arrangement of the ligands at Pt is relatively small, compared with the substantial distortion in d^4 Mo(t-BuS)$_2$(t-BuNC)$_4$. The S–Pt–S angle is even smaller than the right angle, 83.14 (8)°, while the P–Pt–P angle opens up slightly, 97.65 (7)°. This structure is supportive of our conclusion that the large S–Mo–S angle in Mo(t-BuS)$_2$(t-BuNC)$_4$ is due to the d^4 electron count and *cannot* be accounted for by a simple steric argument.

It is interesting to note here that the four extreme orientations of the SH groups (**2**–**5**) in the model d^6 Mo(HS)$_2$(HNC)$_4^{2-}$ molecule are very similar to each other in energy. The calculated relative energies are 0.0 kcal/mol (syn upright, **2**), 0.005 kcal/mol (anti upright, **3**), –0.210 kcal/mol (in-plane I, **4**), and –0.120 kcal/mol (in-plane II, **5**). The energy barriers for going from one conformation to another are also calculated to be practically zero. No wonder that the hydrogen atoms on the SH ligands are crystallographically disordered in the structure of *cis*-Pt(HS)$_2$(Ph$_3$P)$_2$.

Our analysis of the geometrical deformation of Mo(t-BuS)$_2$(t-BuNC)$_4$ differs in detail, yet not in spirit, from the more general discussion of distortions in d^4 six-coordinates complexes.[10] All the tools are in hand for rationalizing or predicting the way in which *any* ligand set will affect the geometry of any six-coordinate complex.

Acknowledgment. K.T. and R.H. thank the National Science Foundation for partial support of this work through research Grant CHE 7828048.

Appendix

All calculations were performed by using the extended Hückel method.[21] The parameters used are listed in Table VII. The values for the H_{ii}'s and orbital exponents were taken from previous work.[10] The parameters for H, C, N, and S are the standard ones.[21] The following bond distances were used: Mo–C, 2.080 Å; Mo–S, 2.373 Å; C–N, 1.159 Å; N–H, 1.030 Å; S–H, 1.340 Å.

Supplementary Material Available: Listing of structure factor tables for Mo(t-BuS)$_2$(t-BuNC)$_4$ (3 pages). Ordering information is given on any current masthead page.

Table VII. Extended Hückel Parameters

orbital	H_{ij}, eV	exponents ζ_1	exponents ζ_2	coeff[a] C_1	coeff[a] C_2
Mo 4d	−11.06	4.54	1.90	0.5899	0.5899
5s	−8.77	1.96			
5p	−5.60	1.90			
H 1s	−13.6	1.300			
C 2s	−21.4	1.625			
2p	−11.4	1.625			
N 1s	−26.0	1.950			
2p	−13.4	1.950			
S 3s	−20.0	1.817			
3p	−13.3	1.817			

[a] These are the coefficients of the exponentials in a double ζ expansion.

(20) Briant, C. E.; Hughes, G. R.; Minshall, P. C.; Mingos, D. M. P. *J. Organomet. Chem.* **1980**, *202*, C18–C20.

(21) Hoffmann, R. *J. Chem. Phys.* **1963**, *39*, 1397–1412. Hoffmann, R.; Lipscomb, W. N. *Ibid.* **1962**, *36*, 2179–2195; **1962**, *37*, 2872–2883.